JACS
JOURNAL OF THE AMERICAN CHEMICAL SOCIETY

Communication

pubs.acs.org/JACS

A Facile Planar Fused-Ring Electron Acceptor for As-Cast Polymer Solar Cells with 8.71% Efficiency

Yuze Lin,[†,‡,§] Qiao He,[†] Fuwen Zhao,[§] Lijun Huo,[⊥] Jiangquan Mai,[∥] Xinhui Lu,[∥] Chun-Jen Su,[¶] Tengfei Li,[†] Jiayu Wang,[†] Jingshuai Zhu,[‡] Yanming Sun,*[,⊥] Chunru Wang,[§] and Xiaowei Zhan*[,†]

[†]Department of Materials Science and Engineering, College of Engineering, Key Laboratory of Polymer Chemistry and Physics of Ministry of Education, Peking University, Beijing 100871, China

[‡]Department of Chemistry, Capital Normal University, Beijing 100048, China

[§]Institute of Chemistry, Chinese Academy of Sciences, Beijing 100190, China

[⊥]Heeger Beijing Research and Development Center, School of Chemistry and Environment, Beihang University, Beijing 100191, China

[∥]Department of Physics, The Chinese University of Hong Kong, New Territories, Hong Kong, China

[¶]National Synchrotron Radiation Research Center, 101 Hsin-Ann Road, Hsinchu Science Park, Hsinchu, Taiwan 30076, China

Supporting Information

ABSTRACT: A planar fused-ring electron acceptor (IC-C6IDT-IC) based on indacenodithiophene is designed and synthesized. IC-C6IDT-IC shows strong absorption in 500−800 nm with extinction coefficient of up to 2.4×10^5 M^{-1} cm^{-1} and high electron mobility of 1.1×10^{-3} cm^2 V^{-1} s^{-1}. The as-cast polymer solar cells based on IC-C6IDT-IC without additional treatments exhibit power conversion efficiencies of up to 8.71%.

For high-performance bulk heterojunction (BHJ) polymer solar cells (PSCs),[1−3] fused-ring electron acceptors (FREAs) have been a promising alternative of fullerenes and their derivatives as electron acceptors.[4] So far, considerable efforts have been dedicated to the development of FREAs[4,5] to overcome insufficiencies of fullerenes, such as weak absorption in the visible spectral region and limited energy level variability. So far, FREA-based PSCs have shown power conversion efficiencies (PCEs) of up to 7−8%,[6−12] which are still lower than those of fullerene counterparts (up to 10−11%).[13−16] Rylene diimides and their derivatives were most widely investigated molecular systems of FREAs.[17,18] Since Zhan et al. reported a perylene diimide (PDI)-based polymer acceptor in 2007,[19] some FREAs based on PDI or naphthalene diimide (NDI) have shown relatively good performance in PSCs;[20−28] and very recently, PSCs based on rylene-based FREAs yielded promising PCEs exceeding 8%.[3,5−7] Most of high-performance PDI and NDI-based FREAs have twisted backbones to decrease the planarity, self-aggregation, and cystalline domains of simple rylene diimides. Besides rylene-based FREAs, electron-donating extended fused rings, e.g., indacenodithiophene (IDT) and indacenodithieno[3,2-*b*]thiophene (IDTT), were tailored by end-capping electron-deficient groups and used as electron acceptors.[29−33] In contrast to rylene diimide-based FREAs which were usually synthesized by multistep reactions, FREAs based on electron-donating extended fused rings with acceptor-donor-acceptor (A-D-A) structure can be easily synthesized by simple reactions. Moreover, their optical and electronic properties, such as absorption and energy levels, can be easily tuned by varying the end-capping electron-withdrawing groups. Now A-D-A FREAs based on extended fused-rings demonstrate promising performance with PCEs of ∼7%.[12,29]

Most of high-performance BHJ solar cells including FREA-based PSCs need additional complicated treatments of their active layers, such as hot spin coating, thermal annealing, solvent additive processing, and solvent vapor annealing, to optimize the morphology. These complicated treatments are not favorable and compatible with the simple, low-cost industry-scale production of large area solar cells. Thus, it is highly urgent and desirable to develop high-performance PSCs based on as-cast films without additional treatments, which depend on the intrinsic morphologic miscibility between donors and acceptors in active layers. To date, the highest PCE of FREA-based PSCs without any extra treatment is 7.39%,[7] and very limited as-cast FREA-based PSCs showed PCEs >6%.

Here, we designed and synthesized a planar IDT-based FREA with four *n*-hexyl side chains (IC-C6IDT-IC, Figure 1a) using one-step facile reaction from commercial available starting materials in high yield. The backbone of IC-C6IDT-IC is highly planar (Figure S1), which is different from the twisted backbone of rylene diimide-based acceptors. IC-C6IDT-IC possesses strong absorption in the 500−800 nm region (the maximum photon density of solar spectra) and high electron mobility in the film. The as-cast PSCs based on IC-C6IDT-IC without additional treatments yield PCEs of up to 8.71%, which is the highest value for fullerene-free PSCs so far and much higher than those (<7.4%) reported for as-cast fullerene-free PSCs, and even higher than those of most as-cast fullerene-based PSCs.

Compound IC-C6IDT-IC was synthesized by one-step simple Knoevenagel condensation of C6IDT-2CHO and INCN in 85% yield (Scheme S1). IC-C6IDT-IC has good

Received: January 24, 2016
Published: February 24, 2016

DOI: 10.1021/jacs.6b00853
J. Am. Chem. Soc. 2016, 138, 2973−2976

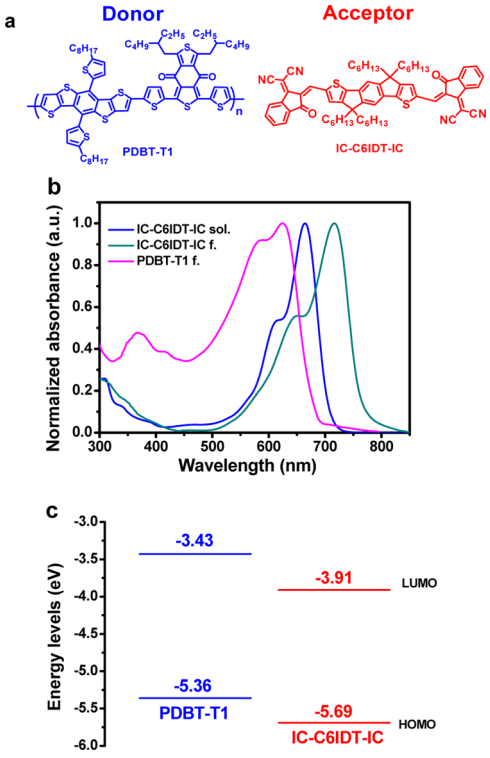

Figure 1. (a) Chemical structures, (b) absorption (sol.: in dichloromethane solution (10^{-6} M); f.: in neat thin film), and (c) energy levels of PDBT-T1 and IC-C6IDT-IC.

solubility in common organic solvents such as chloroform and *o*-dichlorobenzene. The dichloromethane solution (10^{-6} M) of IC-C6IDT-IC exhibits strong absorption in 500−800 nm region with a very high maximum extinction coefficient of 2.4×10^5 M^{-1} cm^{-1} at 664 nm. In the thin film, IC-C6IDT-IC exhibits the maximum absorption peak at 716 nm, which red shifts 52 nm relative to its solution. The optical band gap of IC-C6IDT-IC film is 1.62 eV estimated from the absorption edge (765 nm). This strong and broad absorption of IC-C6IDT-IC benefits the J_{SC} enhancement in PSC. IC-C6IDT-IC has LUMO (−3.91 eV) and HOMO (−5.69 eV) energy levels, estimated from cyclic voltammetry (CV) method (Figure S2), which can match those of some typical high-performance polymer donors. The relatively high electron mobility of IC-C6IDT-IC (1.1×10^{-3} cm^2 V^{-1} s^{-1}) is extracted from space charge limited current measurement from electron-only devices (Figure S3), which is very close to those (10^{-3} cm^2 V^{-1} s^{-1}) of fullerene acceptors and ensures effective charge carrier transport to the electrodes.

To demonstrate potential applications of IC-C6IDT-IC in PSCs as an electron acceptor, we blended it with our previously reported polymer donor PDBT-T1 (Figure 1a)[34] and fabricated BHJ PSCs with a device structure of ITO/ZnO/PDBT-T1: IC-C6IDT-IC/MoO_x/Ag. PDBT-T1 and IC-C6IDT-IC have complementary absorption (Figure 1b) and matched energy levels (Figure 1c, calculated from CV method).[34] Table 1 summarizes open-circuit voltage (V_{OC}), short-circuit current density (J_{SC}), fill factor (FF), and PCE of PSCs at different donor/acceptor (D/A) weight ratios. When the D/A ratio is 1:1, as-cast PSCs show the best performance (Figure 2a): V_{OC} of 0.89 V, J_{SC} of 15.05 mA cm^{-2}, FF of 0.65, and PCE of 8.71% (average PCE over 20 devices: 8.57%). The incident photon to converted current efficiency (IPCE) spectrum of devices is

Table 1. Device Data of PSCs Based on PDBT-T1: IC-C6IDT-IC under the Illumination of AM 1.5 G, 100 mW cm^{-2}

D:A (w/w)	V_{OC} (V)	J_{SC} (mA cm^{-2})	FF	PCE (%)[a]
1.2:1	0.89	14.61	0.63	8.19 (8.11)
1:1	0.89	15.05	0.65	8.71 (8.52)
1:1.3	0.90	14.21	0.61	7.80 (7.69)

[a]Average PCEs in brackets for over 20 devices.

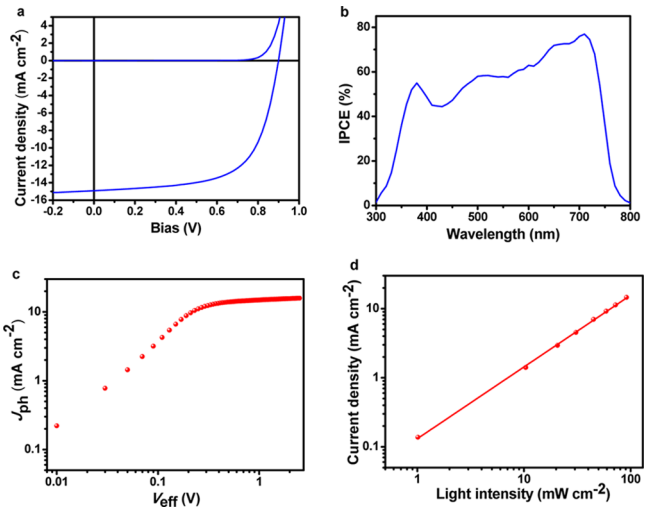

Figure 2. (a) J−V curves, (b) IPCE spectrum, (c) J_{ph} versus V_{eff} characteristics, and (d) J versus light intensity of as-cast devices with the structure ITO/ZnO/PDBT-T1: IC-C6IDT-IC (1:1, w/w)/MoO_x/Ag without any additional treatments.

shown in Figure 2b, as-cast BHJ films exhibit the maximum IPCE of 76% at 710 nm. The calculated J_{SC} obtained from the integration of the IPCE spectrum with the AM 1.5G reference spectrum is 14.68 mA cm^{-2}, which has 2.5% mismatch with that from J−V measurement (15.05 mA cm^{-2}). The broad IPCE plateau spectrum from 350 to 780 nm suggests that both polymer and acceptor make considerable contribution to IPCE and J_{SC}. We investigate the initial stability of the best device under continuous heating at 100 °C. After heating at 100 °C for 1 h, the device PCE decreases ∼16% and then keeps almost stable (Figure S4).

To understand the main mechanism involved in this FREA-based PSC, the charge generation and extraction properties were studied. We measured the photocurrent density (J_{ph}) versus the effective voltage (V_{eff}) of the cells (Figure 2c). J_{ph} can be defined as $J_{ph} = J_L - J_D$, where J_L and J_D are the photocurrent densities under illumination and in the dark, respectively. V_{eff} can be defined as $V_{eff} = V_0 - V_{bias}$, where V_0 is the voltage at which the photocurrent is zero and V_{bias} is the applied external voltage bias. Therefore, V_{eff} determines the electric field in the bulk region and thereby affects the carrier transport and the photocurrent extraction. At high V_{eff} values, mobile charge carriers rapidly move toward the corresponding electrodes with minimal recombination. J_{ph} reaches saturation (15.8 mA cm^{-2}) at $V_{eff} \geq 2.3$ V, suggesting that all photogenerated charge carriers are extracted by the electrodes. Under short-circuit condition, J_{ph} is 14.9 mA cm^{-2}, which is comparable to the saturation J_{ph}. Near the maximum power output point, recombination will be strongly competing with the carrier extraction as carriers slow down due to the reduced electric

DOI: 10.1021/jacs.6b00853
J. Am. Chem. Soc. 2016, 138, 2973−2976

field. However, the J_{ph} is still as high as 12.5 mA cm^{-2} at the maximum power output point, which is ~79% of all photogenerated carriers collected by the electrodes, indicating efficient photogenerated exciton dissociation and charge collection.[34−36]

We also measured current under different light intensities to study charge recombination under the short circuit condition (Figure 2d). The relationship between J_{SC} and light intensity (P) can be described by the formula of $J_{SC} \propto P^S$. If all free carriers are swept out and collected at the electrodes prior to recombination, S should be equal to 1, while $S < 1$ indicates some extent of bimolecular recombination.[35−37] The current density shows a linear dependence on the light intensity in logarithmic coordinates with a slope (S) of 1.0, indicative of efficient sweep-out of carriers and neglectable bimolecular recombination.

The surface morphology of the BHJ active layer was examined by atomic force microscopy in the tapping mode. The PDBT-T1: IC-C6IDT-IC blended film shows very smooth and uniform surface (Figure S5) with small root-mean-square roughness of 0.86 nm, which is beneficial to the contact between active layer and top electrode. The molecular packing in as-casted PDBT-T1 and IC-C6IDT-IC neat films as well as PDBT-T1: IC-C6IDT-IC blended films was investigated using grazing incident wide-angle X-ray scattering (GIWAXS) measurements.[38] The two-dimensional (2D) GIWAXS patterns of neat IC-C6IDT-IC, neat PDBT-T1, and their blend are shown in Figure 3a−c, and the corresponding intensity profiles

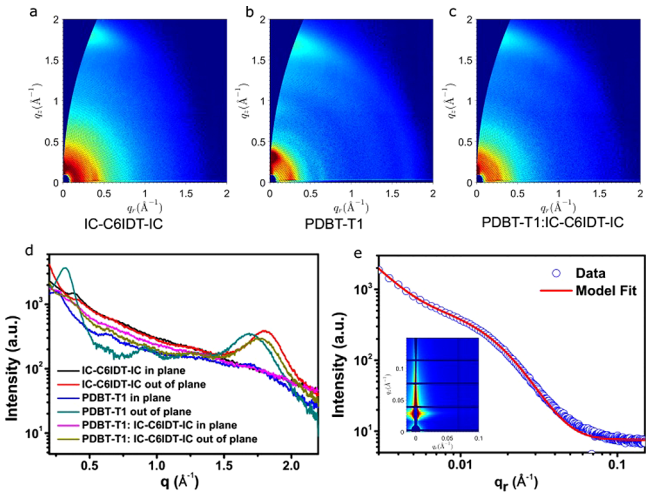

Figure 3. (a−c) 2D GIWAXS patterns and (d) scattering profiles of in-plane and out-of-plane for IC-C6IDT-IC, PDBT-T1, and PDBT-T1: IC-C6IDT-IC (1:1, w/w) blended films. (e) GISAXS profile of PDBT-T1:IC-C6IDT-IC (1:1, w/w) blended film and its model fit (inset: the corresponding GISAXS pattern).

q in the in-plane and out-of-plane direction are plotted in Figure 3d. The (100) lamellar peak of IC-C6IDT-IC locates at q = 0.39 Å^{-1}, corresponding to a lamellar spacing of ~16 Å, while the (100) of PDBT-T1 locates at q = 0.30 Å^{-1} (~20 Å). The average crystallite sizes of IC-C6IDT-IC and PDBT-T1 are 9.2 and 7.8 nm, respectively, estimated from the lamellar peak width via Scherrer equation.[39] Remarkably, obvious out-of-plane $\pi-\pi$ (010) stacking peaks are observed for all the three films at q_z = 1.79 Å^{-1} (IC-C6IDT-IC), 1.68 Å^{-1} (PDBT-T1), and 1.75 Å^{-1} (PDBT-T1: IC-C6IDT-IC), indicating the preservation of strong $\pi-\pi$ stacking order after blending as well molecules are highly ordered with preferential "face-on" orientation with respect to the electrode substrates. This explains the relatively good vertical charge transport (hole mobility: 5.1 × 10^{-5} cm^2 V^{-1} s^{-1}, electron mobility: 2.9 × 10^{-4} cm^2 V^{-1} s^{-1}) in the blended films (Figures S6 and S7).

The nanoscale phase separation within the blended film was investigated by grazing-incidence small-angle X-ray scattering (GISAXS) measurements.[40,41] Figure 3e presents the 2D GISAXS pattern and in-plane intensity profile of the blended film, while the neat film data are shown in Figure S8. The neat IC-C6IDT-IC film demonstrates a power law scattering $\propto q^{-4}$, indicating that IC-C6IDT-IC crystallites disperse randomly in the amorphous domains. In contrast, the neat PDBT-T1 film exhibits an apparent shoulder in the intermediate q regime, signifying the aggregation of polymer crystallites. Hence, we fit the scattering profile of blended film by considering the contributions from (1) amorphous intermixing domains and (2) aggregated crystalline polymer domains with the models adopted by Liao et al.[40] From the fitting results, we can estimate that the amorphous domain size is ~45 nm and the aggregated crystalline polymer domain size is ~23 nm. These length scales are comparable to the theoretical exciton diffusion length,[42] thereby beneficial to effective charge separation.

In summary, a planar FREA (IC-C6IDT-IC) was designed and synthesized by one-step facile reaction of two commercial available starting materials in a high yield. IC-C6IDT-IC possesses strong and complementary absorption in 500−800 nm range and matched energy levels with PDBT-T1 donor as well as high electron mobility. The as-cast PDBT-T1: IC-C6IDT-IC blended film shows very smooth surface, strong "face-on" $\pi-\pi$ ordering and appropriate phase separation scale, and relatively good charge transport. The as-cast PSC based on PDBT-T1: IC-C6IDT-IC blend shows efficient excition dissociation and neglectable bimolecular recombination. The as-cast PSCs yield PCEs of up to 8.71%, which is the highest value for fullerene-free PSCs, and much higher than those of as-cast fullerene-free PSCs (<7.4%). The traditional opinion on FREAs is that they must have twisted backbones to suppress self-aggregation and large phase separation and to promote donor/acceptor miscibility, exemplified by rylene diimide-based acceptors. Our planar acceptor IC-C6IDT-IC with good planarity exhibits much better performance in as-cast PSCs than the twisted rylene diimide-based acceptors. Our results challenge the traditional opinion on design of FREAs and demonstrate that planar electron acceptors can exhibit very promising performance in PSCs and should deserve further attention.

■ ASSOCIATED CONTENT

Supporting Information

The Supporting Information is available free of charge on the ACS Publications website at DOI: 10.1021/jacs.6b00853.

Experimental details and data (PDF)

■ AUTHOR INFORMATION

Corresponding Authors

*xwzhan@pku.edu.cn

*sunym@buaa.edu.cn

Notes

The authors declare no competing financial interest.

DOI: 10.1021/jacs.6b00853
J. Am. Chem. Soc. 2016, 138, 2973−2976

■ ACKNOWLEDGMENTS

This work was supported by the 973 Program (2013CB834702), NSFC (91433114, 51261130582, 21504058), and the International Science & Technology Cooperation Program of China (no. 2014DFA52820). The Supercomputing Center of Chinese Academy of Sciences is acknowledged for molecular modeling.

■ REFERENCES

(1) Li, Y. *Acc. Chem. Res.* **2012**, *45*, 723.
(2) Cheng, Y.-J.; Yang, S.-H.; Hsu, C.-S. *Chem. Rev.* **2009**, *109*, 5868.
(3) Lu, L.; Zheng, T.; Wu, Q.; Schneider, A. M.; Zhao, D.; Yu, L. *Chem. Rev.* **2015**, *115*, 12666.
(4) Lin, Y.; Zhan, X. *Adv. Energy Mater.* **2015**, *5*, 1501063.
(5) Lin, Y.; Zhan, X. *Mater. Horiz.* **2014**, *1*, 470.
(6) Zhong, Y.; Trinh, M. T.; Chen, R.; Purdum, G. E.; Khlyabich, P. P.; Sezen, M.; Oh, S.; Zhu, H.; Fowler, B.; Zhang, B.; Wang, W.; Nam, C.-Y.; Sfeir, M. Y.; Black, C. T.; Steigerwald, M. L.; Loo, Y.-L.; Ng, F.; Zhu, X. Y.; Nuckolls, C. *Nat. Commun.* **2015**, *6*, 8242.
(7) Meng, D.; Sun, D.; Zhong, C.; Liu, T.; Fan, B.; Huo, L.; Li, Y.; Jiang, W.; Choi, H.; Kim, T.; Kim, J. Y.; Sun, Y.; Wang, Z.; Heeger, A. J. *J. Am. Chem. Soc.* **2016**, *138*, 375.
(8) Hwang, Y.-J.; Li, H.; Courtright, B. A. E.; Subramaniyan, S.; Jenekhe, S. A. *Adv. Mater.* **2016**, *28*, 124.
(9) Hwang, Y.-J.; Courtright, B. A. E.; Ferreira, A. S.; Tolbert, S. H.; Jenekhe, S. A. *Adv. Mater.* **2015**, *27*, 4578.
(10) Gao, L.; Zhang, Z.-G.; Xue, L.; Min, J.; Zhang, J.; Wei, Z.; Li, Y. *Adv. Mater.* **2015**, DOI: 10.1002/adma.201504629.
(11) Kwon, O. K.; Uddin, M. A.; Park, J.-H.; Park, S. K.; Nguyen, T. L.; Woo, H. Y.; Park, S. Y. *Adv. Mater.* **2016**, *28*, 910.
(12) Lin, H.; Chen, S.; Li, Z.; Lai, J. Y. L.; Yang, G.; McAfee, T.; Jiang, K.; Li, Y.; Liu, Y.; Hu, H.; Zhao, J.; Ma, W.; Ade, H.; Yan, H. *Adv. Mater.* **2015**, *27*, 7299.
(13) Liu, Y. H.; Zhao, J. B.; Li, Z. K.; Mu, C.; Ma, W.; Hu, H. W.; Jiang, K.; Lin, H. R.; Ade, H.; Yan, H. *Nat. Commun.* **2014**, *5*, 5293.
(14) Huo, L.; Liu, T.; Sun, X.; Cai, Y.; Heeger, A. J.; Sun, Y. *Adv. Mater.* **2015**, *27*, 2938.
(15) Ouyang, X.; Peng, R.; Ai, L.; Zhang, X.; Ge, Z. *Nat. Photonics* **2015**, *9*, 520.
(16) Zhang, J.; Zhang, Y.; Fang, J.; Lu, K.; Wang, Z.; Ma, W.; Wei, Z. *J. Am. Chem. Soc.* **2015**, *137*, 8176.
(17) Guo, X.; Facchetti, A.; Marks, T. J. *Chem. Rev.* **2014**, *114*, 8943.
(18) Zhan, X.; Facchetti, A.; Barlow, S.; Marks, T. J.; Ratner, M. A.; Wasielewski, M. R.; Marder, S. R. *Adv. Mater.* **2011**, *23*, 268.
(19) Zhan, X.; Tan, Z. a.; Domercq, B.; An, Z.; Zhang, X.; Barlow, S.; Li, Y.; Zhu, D.; Kippelen, B.; Marder, S. R. *J. Am. Chem. Soc.* **2007**, *129*, 7246.
(20) Zhang, X.; Lu, Z.; Ye, L.; Zhan, C.; Hou, J.; Zhang, S.; Jiang, B.; Zhao, Y.; Huang, J.; Zhang, S.; Liu, Y.; Shi, Q.; Liu, Y.; Yao, J. *Adv. Mater.* **2013**, *25*, 5791.
(21) Liu, Y.; Mu, C.; Jiang, K.; Zhao, J.; Li, Y.; Zhang, L.; Li, Z.; Lai, J. Y. L.; Hu, H.; Ma, T.; Hu, R.; Yu, D.; Huang, X.; Tang, B. Z.; Yan, H. *Adv. Mater.* **2015**, *27*, 1014.
(22) Lin, Y.; Wang, Y.; Wang, J.; Hou, J.; Li, Y.; Zhu, D.; Zhan, X. *Adv. Mater.* **2014**, *26*, 5137.
(23) Jung, J. W.; Jo, J. W.; Chueh, C. C.; Liu, F.; Jo, W. H.; Russell, T. P.; Jen, A. K. Y. *Adv. Mater.* **2015**, *27*, 3310.
(24) Sun, D.; Meng, D.; Cai, Y.; Fan, B.; Li, Y.; Jiang, W.; Huo, L.; Sun, Y.; Wang, Z. *J. Am. Chem. Soc.* **2015**, *137*, 11156.
(25) Li, H. Y.; Earmme, T.; Ren, G. Q.; Saeki, A.; Yoshikawa, S.; Murari, N. M.; Subramaniyan, S.; Crane, M. J.; Seki, S.; Jenekhe, S. A. *J. Am. Chem. Soc.* **2014**, *136*, 14589.
(26) Hartnett, P. E.; Timalsina, A.; Matte, H. S. S. R.; Zhou, N.; Guo, X.; Zhao, W.; Facchetti, A.; Chang, R. P. H.; Hersam, M. C.; Wasielewski, M. R.; Marks, T. J. *J. Am. Chem. Soc.* **2014**, *136*, 16345.
(27) Facchetti, A. *Mater. Today* **2013**, *16*, 123.
(28) Pho, T. V.; Toma, F. M.; Chabinyc, M. L.; Wudl, F. *Angew. Chem., Int. Ed.* **2013**, *52*, 1446.
(29) Lin, Y.; Wang, J.; Zhang, Z.; Bai, H.; Li, Y.; Zhu, D.; Zhan, X. *Adv. Mater.* **2015**, *27*, 1170.
(30) Lin, Y.; Zhang, Z.; Bai, H.; Wang, J.; Yao, Y.; Li, Y.; Zhu, D.; Zhan, X. *Energy Environ. Sci.* **2015**, *8*, 610.
(31) Wu, Y.; Bai, H.; Wang, Z.; Cheng, P.; Zhu, S.; Wang, Y.; Ma, W.; Zhan, X. *Energy Environ. Sci.* **2015**, *8*, 3215.
(32) Holliday, S.; Ashraf, R. S.; Nielsen, C. B.; Kirkus, M.; Röhr, J. A.; Tan, C.-H.; Collado-Fregoso, E.; Knall, A.-C.; Durrant, J. R.; Nelson, J.; McCulloch, I. *J. Am. Chem. Soc.* **2015**, *137*, 898.
(33) Lin, Y.; Zhan, X. *Acc. Chem. Res.* **2016**, *49*, 175.
(34) Huo, L.; Liu, T.; Sun, X.; Cai, Y.; Heeger, A. J.; Sun, Y. *Adv. Mater.* **2015**, *27*, 2938.
(35) Zhao, J. B.; Li, Y. K.; Lin, H. R.; Liu, Y. H.; Jiang, K.; Mu, C.; Ma, T. X.; Lai, J. Y. L.; Hu, H. W.; Yu, D. M.; Yan, H. *Energy Environ. Sci.* **2015**, *8*, 520.
(36) Lu, L.; Xu, T.; Chen, W.; Landry, E. S.; Yu, L. *Nat. Photonics* **2014**, *8*, 716.
(37) Zang, Y.; Li, C. Z.; Chueh, C. C.; Williams, S. T.; Jiang, W.; Wang, Z. H.; Yu, J. S.; Jen, A. K. Y. *Adv. Mater.* **2014**, *26*, 5708.
(38) Lu, X.; Hlaing, H.; Germack, D. S.; Peet, J.; Jo, W. H.; Andrienko, D.; Kremer, K.; Ocko, B. M. *Nat. Commun.* **2012**, *3*, 795.
(39) Smilgies, D. M. *J. Appl. Crystallogr.* **2013**, *46*, 286.
(40) Liao, H.-C.; Tsao, C.-S.; Shao, Y.-T.; Chang, S.-Y.; Huang, Y.-C.; Chuang, C.-M.; Lin, T.-H.; Chen, C.-Y.; Su, C.-J.; Jeng, U. S.; Chen, Y.-F.; Su, W.-F. *Energy Environ. Sci.* **2013**, *6*, 1938.
(41) Liao, H.-C.; Tsao, C.-S.; Lin, T.-H.; Chuang, C.-M.; Chen, C.-Y.; Jeng, U. S.; Su, C.-H.; Chen, Y.-F.; Su, W.-F. *J. Am. Chem. Soc.* **2011**, *133*, 13064.
(42) Liu, F.; Gu, Y.; Wang, C.; Zhao, W.; Chen, D.; Briseno, A. L.; Russell, T. P. *Adv. Mater.* **2012**, *24*, 3947.

DOI: 10.1021/jacs.6b00853
J. Am. Chem. Soc. 2016, 138, 2973−2976